Journal of Applied Fluid Mechanics, Vol. 13, No. 2, pp. 401-412, 2020.
Available online at www.jafmonline.net, ISSN 1735-3572, EISSN 1735-3645.
DOI: 10.29252/jafm.13.02.30347

Performance Comparison of Novel Single and Bi-Diaphragm PZT Based Valveless Micropumps

H. Asadi Dereshgi[1†], M. Z. Yildiz[2] and N. Parlak[3]

[1] *Mechatronics Engineering, Institute of Natural Sciences, Sakarya University, Sakarya, 54050, Turkey*
[2] *Department of Electrical and Electronics Engineering, Sakarya University of Applied Sciences, Sakarya, 54050, Turkey*
[3] *Department of Mechanical Engineering, Sakarya University, Sakarya, 54050, Turkey*

†*Corresponding Author Email: hamid.dereshgi@ogr.sakarya.edu.tr*

(Received April 4, 2019; accepted July 13, 2019)

ABSTRACT

A commercial micropump should provide properties that justify the simple structure and miniaturization, high reliability, simple working principle, low cost and no need for complex controller. In this study, two novel piezoelectric actuated (lead zirconate titanate-PZT) valveless micropumps that can achieve high flow rates by pumping chambers and fixed reservoirs were designed and fabricated. Extensive experiments were conducted to investigate the effects of hydrodynamic and electromechanical on flow rates of the Single Diaphragm Micropump (SDM) and the Bi-diaphragm Micropump (BDM). BDM had two actuators facing to the same chamber at 180-degree phase shift. The primary features of the proposed designs were the high flow rates at low driving voltages and frequencies with the help of innovative design geometry. 3D-printing technique providing one-step fabrication for integrated micropumps with fixed reservoir was used. The micropump materials were biocompatible and can be used repeatedly to reduce costs. Mechanical parameters such as tensile test for silicon diaphragm, surface topography scanning by microscopy techniques and drop shape analysis for hydrophobic property were investigated to reveal surface wetting and flow stability. In addition, the effect of reservoir height was investigated and the calibration flow rates were measured during the inactive periods. The maximum diaphragm displacements were obtained at 45 V and 5 Hz. The maximum flow rate of SDM and BDM at 45 V and 20 Hz were 32.85 ml/min and 35.4 ml/min respectively. At all driving voltage and frequency levels, BDM had higher flow rates than of SDM.

Keywords: Valveless micropump; Bi-diaphragm; Piezoelectric actuators; Fluid flow measurement; Displacement measurement.

NOMENCLATURE

D	diameter	v	fluid velocity
f	darcy friction factor	z	height
g	acceleration of gravity		
K	loss coefficient	Δh_{total}	total head loss
L	length	ρ	density
P	pressure		

1. INTRODUCTION

In the past few decades, the advances in micro-electro-mechanical systems (MEMS) technologies have contributed to the rapid development of microfluidic devices in various functions (Wang *et al.*, 2018). One of the important elements on MEMS is the micropump, which is capable of producing flow rates ranging in milliliter (ml) or microliter (μl) per minute. The first MEMS-based micropump was presented by Smits and Vitafin (1984) for insulin delivery systems to diabetic patients (Smits *et al.*, 1984). Micropumps are classified as either mechanical or non-mechanical types (Tay *et al.*, 2002). Mechanical micropumps contain moving parts such as check valves and diaphragms, while non-mechanical micropumps do not have moving components. The mechanical micropumps require

an actuator vibrate the diaphragm to perform a pump operation. Thus, the fluid suction and discharge operation take place in the micropump (Nisar *et al.*, 2008; Dereshgi *et al.*, 2018a). There are various mechanisms for creating vibrations including; electrostatic (Teymoori *et al.*, 2005), electromagnetic (Lee *et al.*, 2012), thermal pneumatic (Schomburg *et al.*, 1994), shape memory alloy (Chang *et al.*, 2006), phase change (Sim *et al.*, 2003) and piezoelectric (Afrasiab *et al.*, 2011; Kolahdouz *et al.*, 2014; Derakhshan *et al.*, 2019). Among them, the piezoelectrics are quick to operate compared to other actuators. They produce a reasonably intermediate pressure against low energy consumption. Accordingly, the piezoelectric is a good actuator for micropumps that designed for biomedical applications (Dereshgi *et al.*, 2018b; Farshchi Yazdi *et al.*, 2019).

Generally, micropumps have fabricated by common microfabrication technologies with polymethyl methacrylate (PMMA), polydimethylsiloxane (PDMS), pyrex glass and silicon materials (Hsu *et al.*, 2007; Amirouche *et al.*, 2009). The diaphragm separates the fluid from the piezoelectric actuator. Silicon (Cazorla *et al.*, 2016; Dereshgi, 2016), Beryllium bronze (Wang *et al.*, 2016), Polyethylene Terephthalate (PET) (Pabst *et al.*, 2013; Pabst *et al.*, 2014), SU8 (Le *et al.*, 2017), Brass (Dong *et al.*, 2017), Parylene-C (PCPX)-Tetraethyl Orthosilicate (TEOS) (Johnson *et al.*, 2016), Nafion–Pt (Shoji *et al.*, 2016), Earthworm muscle (Tanaka *et al.*, 2017), Polyimide (Hamid *et al.*, 2016), Elastomeric (Robertson *et al.*, 2016), Thermoplastic Polyurethane (TPU) (Shaegh *et al.*, 2015), PDMS (Zhou *et al.*, 2011; Kawun *et al.*, 2016) and Soft Magnetorheological Elastomer (SMRE) (Ehsani *et al.*, 2017) are diaphragm materials that are mainly used in the literature. Maillefer *et al.* (2001) used a silicon diaphragm in a micropump designed for drug delivery, because of its low cost and high performance (Maillefer *et al.*, 2001). Moreover, silicon has features such as high dielectric strength, hydrophobicity, sterilizable, durability (Sardar *et al.*, 2016). Microvalves that are classified as valveless and with check-valve types are one of the most important elements of micropumps. Check-valve type micro-valves can avoid back flow but have a complicated structure. Additionally, there is a risk of valvular erosion and valve blockage by small particles or bubbles in liquids. Valveless type micro-valves cannot fully control the back flow and clogging, but their structure is simple comparing to check-valves (Mohammadzadeh *et al.*, 2013; Revathi *et al.*, 2018). Literature survey shows that there are many studies about the piezoelectric actuated diaphragm micropumps. For example, Zhang *et al.* (2013a) in other studies, a single piezoelectric diaphragm micropump was fabricated and used check valves in the entrance and exit of the chamber. In the presented study, the effects of voltages and frequencies that cause flow rate changes on the micropump were investigated. Therefore, the piezoelectric actuator was divided into two parts as driving unit and sensing unit. However, they did not report that use any isolating diaphragm between the piezoelectric actuator and water. The maximum flow rate was 45.98 ml/min which obtained at 150 V_{p-p} and 30 Hz, additionally, the sensing voltage achieves a maximum value of 3.02 V_{p-p}. In addition, Zhang *et al.* (2013b) presented a prototype micropump with double piezoelectric diaphragm which serial connected. The size of the prototype micropump was 65mm × 40mm × 12 mm. They showed that the advantages of double actuator micropumps and maximum flow rate in prototype micropump was 45.98 ml/min which obtained at 200 V and 15 Hz. For fuel delivery applications, Wang *et al.* (2014) fabricated a check valve micropump was composed of three parts, namely, piezoelectric actuator, chamber and valves. The novelty of this work consists of compressible spaces made of PMMA plate that was mounted at the bottom of the micropump. As a result, the compressible spaces caused to increase flow rate. The maximum flow rate of 105 ml/min were obtained when the piezoelectric actuator was driven with 400 V_{p-p} and 490 Hz. Ma *et al.* (2015a) reported a piezoelectric-based micropump for biomedical applications. They designed the chamber in the form of rib structures to direct the flow. Consequently, the maximum flow rate was reported as 196 ml/min at 70 V and 25 Hz. Ma *et al.* (2015b) designed low flow piezoelectric micropump with check valves. The chamber was fabricated from the PMMA and the diameter was 10 mm. The important highlight of this study was the new diaphragm model that fabricated a cylindrical protrusion had clamped to the center of the micropump's PDMS diaphragm. Additionally, the effects of chamber depth and diaphragm thickness on flow rate were investigated. As a result, the maximum obtained flow rate was 6.21 ml/min. Pan *et al.* (2015) studied on the same micropump done by Wang *et al.* (2014). However, in this study a square wave voltage and sinusoidal wave voltage were used to drive the piezoelectric actuator. Consequently, the performance of this micropump at the square wave voltage was much better than the sinusoidal wave voltage. Thus, the maximum flow rate was 163.7 ml/min when the piezoelectric actuator was driven with a square-wave voltage of 400 V_{p-p} and 445.5 Hz. In another study of Ma *et al.* (2016) designed the valveless piezoelectric micropump for biomedical applications. The only difference was that the vibrator of the micropump was a piezoelectric bimorph actuator connecting with Polyethylene Terephthalate (PET) diaphragm. The maximum flow rate was 9.1 ml/min. The paper of Okura *et al.* (2017) reported a microfluidic droplet creation device consisting of a PDMS microfluidic chip in the field of drug delivery. The maximum flow rate of this micropump was reported as 10 ml/min at 250 V_{p-p} and 60 Hz. Eventually, Ye *et al.* (2018) fabricated a new micropump design by adding a thin steel blocking edge which was pressed perpendicularly to the center of the check valve film. They reported that the flow rate increased by 40% - 300% and the maximum flow rate was obtained 187.2 ml/min.

Many studies have been carried out on micro pumps. However, none of them contain detailed information about design parameters, mechanical

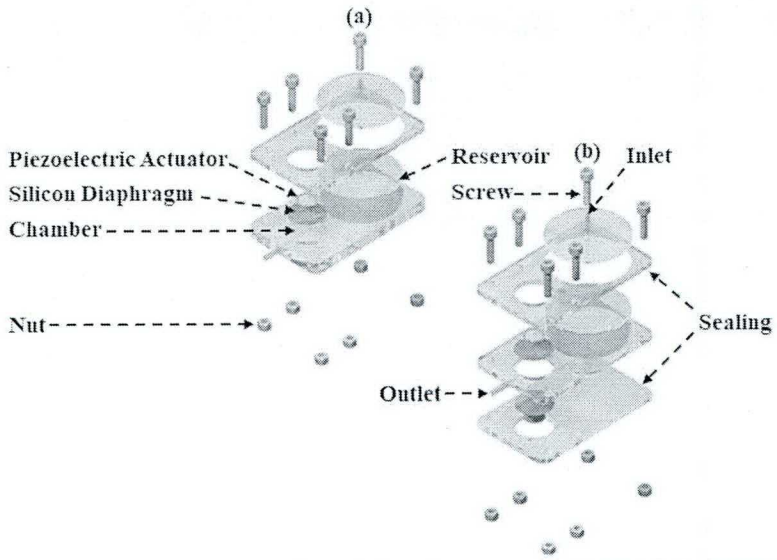

Fig. 1. Exploded view of the micropumps, (a) SDM, (b) BDM.

and electrical effects on flow rates. In addition, new designs have been proposed by different researchers, but there are no studies supporting each other.

In this study, we fabricated two PZT based novel micropumps that can be used in a wide range of areas such as mechanical, energy and biomedical applications. The novelty of this study was that the BDM (Bi-diaphragm Micropump) and SDM (Single Diaphragm Micropump) had a fixed reservoir near the chamber to achieve portable and controllable features. Another geometric novelty was that the BDM consisted of a chamber sandwiched between two diaphragms actuated by two piezoelectric actuators at the same time to achieve high flow rate.

According to literature survey, there is no similar micropump geometry in the presented studies. In order to compare the performance of the BDM, we fabricated the SDM with same geometric parameters and material. All the structure elements of the micropumps were selected as biocompatible. Therefore, the silicon was chosen as a diaphragm in these micropumps, and the PMMA was used to fabricate the chamber, nozzle/diffuser elements and reservoir. Profilometer, Scanning Electron Microscopy and Field Emission Microscopy were used for surface roughness characteristics of the fabricated micropumps. Drop shape analysis was used to test hydrophobic or hydrophilic behavior of the PMMA material. At last, a tensile test was applied for elastic behavior of the silicon diaphragm. Consequently, experimental flow rates were measured and it was shown that BDM had higher flow rates at all frequency and voltage levels.

2. MATERIALS AND METHODS

2.1 Micropump Design and Working Principle

The structure of piezoelectric micropumps is shown in Fig. 1. These micropumps consist of fluid reservoir, chamber, nozzle/diffuser elements, silicon diaphragm and piezoelectric actuator. We fabricated the chamber, nozzle/diffuser and fluid reservoir in the clean room by using the Objet260 Connex3 printer. The material of these elements was PMMA. On the other hand, in this study, piezoelectric coated brass disks were used, which can be available commercially. Moreover, silicon diaphragm was the separator layer of piezoelectric actuator with water. To study the characteristics of the silicon diaphragm "Tensile Test" was performed. In addition, the silicon diaphragm properties can be summarized as; Young's modulus (162 GPa), Poisson's ratio (0.22) and density (2329 kg/m^3) respectively. The optimum nozzle diffuser divergence angle was reported 10-degrees (Singh *et al.*, 2015). Therefore, in this study the nozzle/diffuser divergence angle was chosen 10-degrees. Inlet and outlet diameters of nozzle-diffuser elements were designed to be 0.2 mm and 2 mm, respectively. The height of the reservoir and radius were 20 mm and 25 mm, respectively. The geometric parameters of the micropumps components were given in the Table 1.

As shown in Fig. 1, the physical parameters of the two micropumps were exactly equal. The only difference between these two micropumps was the number of diaphragm and piezoelectric actuators. Thus, that in the SDM, in the upper part of the chamber, there was a silicon diaphragm and a piezoelectric actuator. While in the BDM, two silicon diaphragm and two piezoelectric actuators were used. Figure 2 shows the prototype micropumps fabricated by PMMA material.

Figure 3 shows the working principle of the proposed micropumps. The working principle and displacement measurement of the represented micropumps in this study were similar to the studies by Mohith *et al.* (2019); Yildiz *et al.* (2019) and Dereshgi *et al.* (2019). Applying alternative voltage

Table 1 Geometrical characteristics of micropumps components

Micropump component	Specifications (mm)
Chamber diameter (d_{Ch})	25
Chamber height (h_{Ch})	4
Nozzle diameter (d_N)	0.2
Diffuser diameter (d_D)	2
Silicon diaphragm diameter (d_S)	25
Silicon diaphragm thickness (t_S)	0.1
Piezoelectric actuator diameter (d_P)	14
Piezoelectric actuator thickness (t_P)	0.2
Reservoir diameter (d_R)	50
Reservoir height (h_R)	20

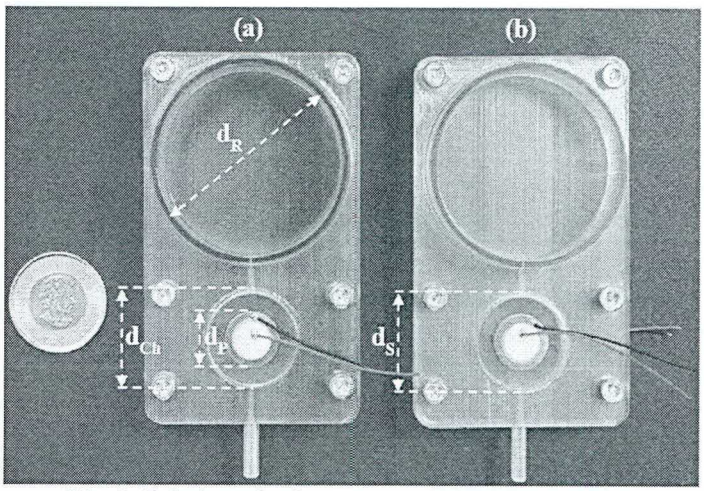

Fig. 2. Fabricated micropumps (a) SDM, (b) BDM.

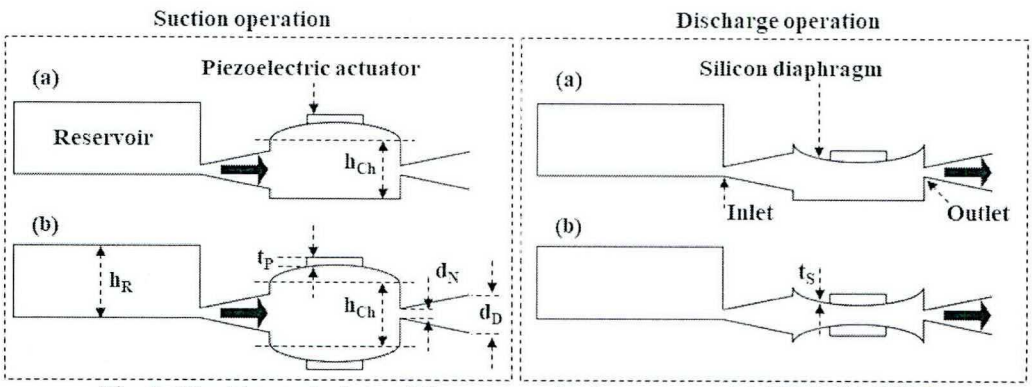

Fig. 3. Working principle of the proposed micropumps, (a) SDM, (b) BDM.

causes piezoelectric deformation that is called reverse piezoelectric effect. The piezoelectric displacement rate depends on the amount of applied voltage and its direction. The diaphragm displacement in piezoelectric micropumps causes the pump stroke to increase and decrease periodically. Thus, the fluid is delivered from the inlet to the outlet. The flow is assumed to be Newtonian, steady, incompressible and fluid with constant properties. The mesh convergence method was used by COMSOL Multiphysics 4.3 to obtain required displacement amplitude of the diaphragm where the values were saturated. The working principle of piezoelectric actuators include two stages, namely, the discharge and the suction. By applying the sinusoidal voltage, the diaphragm vibrates. In the positive half cycle of the sinusoidal voltage, the diaphragm bends upwards, and in this situation, the liquid suction was carried out from the reservoir to the chamber. In the negative half-cycle of the sinusoidal voltage, the diaphragm bends downward and the discharge of fluid from the chamber takes place. In this study, to piezoelectric of both micropumps the same voltage and frequencies were applied. However, the sinusoidal voltage was applied with 180-degrees phase shift to

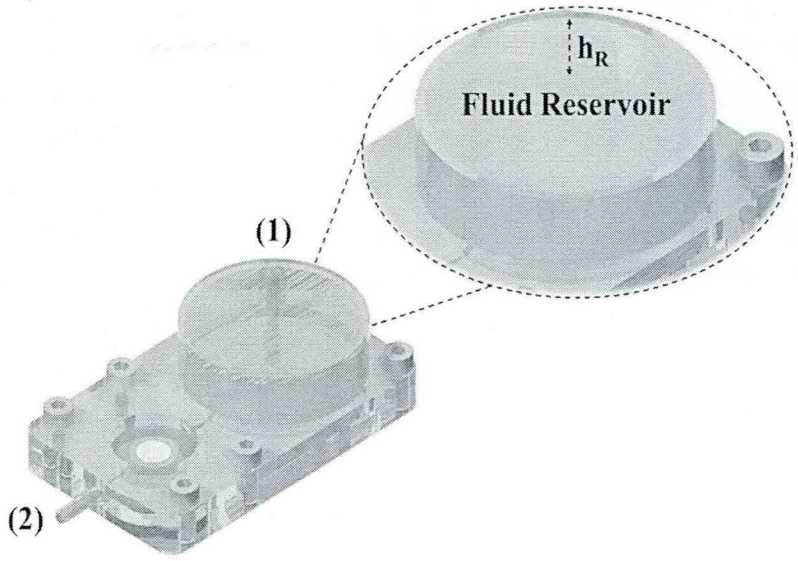

Fig. 4. The effect of reservoir height on flow rate.

BDM's piezoelectric actuators. The phase shift increased the suction and discharge force of the BDM compared to the SDM. In other words, increasing discharge and suction force resulted in an increase in net flow rate. The results obtained from the micropumps are presented in Section 3.

2.2 Micropump Calibration and Flow Test

In this study micropumps and fluid reservoir were fabricated as adjacent as shown in Fig. 4. Each micropump (SDM and BDM) had a fluid reservoir. The micropump chamber was connected with reservoir through a nozzle/diffuser element. The nozzle/diffuser elements did not have moving components. Therefore, when the voltage was not applied to the piezoelectric (inactive status), always a constant amount of flow rate was obtained due to water height in reservoir. Therefore, hydrostatic pressure gradient occurred from reservoir (pointed as 1 in Fig. (4)) to outlet (2) of micro pump and head loss caused by a sudden increase or decrease could be considered in theoretical calculation.

While energy equation was applied for the one-dimensional control volume for not pumping, extended Bernoulli equation is expressed in Eq. (1);

$$\frac{P_1}{\rho g}+\frac{v_1^2}{2g}+z_1=\frac{P_2}{\rho g}+\frac{v_2^2}{2g}+z_2+\Delta h_{total} \quad (1)$$

P: Fluid pressure, v: Fluid Velocity, z: Height of streamline, ρ: Fluid density, g: Gravity constant.

"P_1" and "P_2" are atmospheric pressures, "v_1" and "z_2" are equal to zero. Finally, "Δh_{total}" total head loss is consisted of friction (f) and minor losses,

$$\Delta h_{total}=(f\frac{L}{D}+\Sigma K)\frac{v^2}{2g} \quad (2)$$

where, "L" is the length, "D" is the diameter and "K" is the loss coefficient. In the literature, values of "K" have been studied for Nozzle and diffusers (Stemme *et al.*, 1993; Singhal *et al.*, 2004). Based on literature studies, total head loss was obtained with Eq. (2). Additionally, the theoretical flow rates were calculated according to the liquid height in the reservoir. Then theoretical flow rates are confirmed by the experimental data collected on inactive status. In order to determine the flow rates caused only by PZT, the experiments were repeated while the piezo on active status. The flow tests for SDM and BDM micropumps were performed on active and inactive status and actual piezo flow rates were determined subtracting from each other.

Water has been used as a working fluid in the investigation. In experiments, the fluid (water) was at ambient conditions (20.0 – 21.0 ^{0} C). Mass flow measurement has been done by both from precision glass syringe and measuring water weight collected on a digital balance (Mettler Toledo ML200T). All measurements were repeated at least three times to improve reliability of the flow tests. The analyzed measurement uncertainties were calculated according to the method presented by Kline and McClintock (Holman *et al.*, 2001). Standard deviation of flow rates was calculated and random errors were determined by multiplying by 1.95 for 95% confidence level. Standard uncertainties of measured parameters were: 21 ^{0} C ± 0.6 for inlet temperature; 60 s ± 0.0003 for time interval; 10 g ± 0.01 for digital balance and 999 kg/m^3 ± 0.1 for density of water. As a result, the highest uncertainties of volume and mass flow rate were calculated for tests under conducted 5 V and 5 Hz as ∓ 2.2 % and ∓ 2.3 % respectively.

3. RESULTS

3.1 Drop Shape Analysis (DSA)

Surface roughness, porosity and hydrophilicity are important factors in fluid mechanics because they

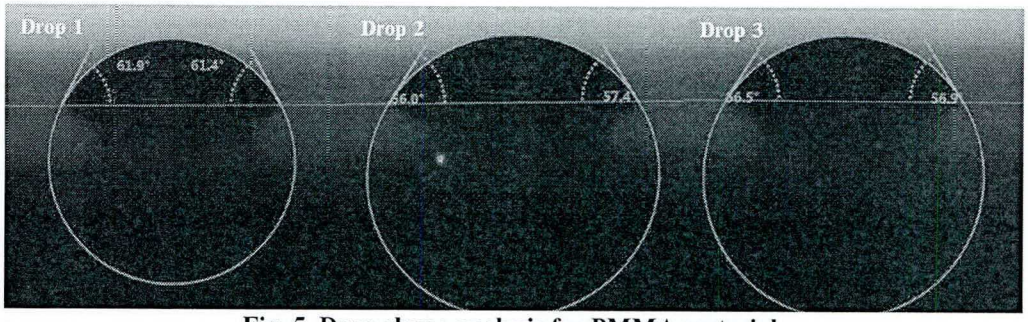

Fig. 5. Drop shape analysis for PMMA material.

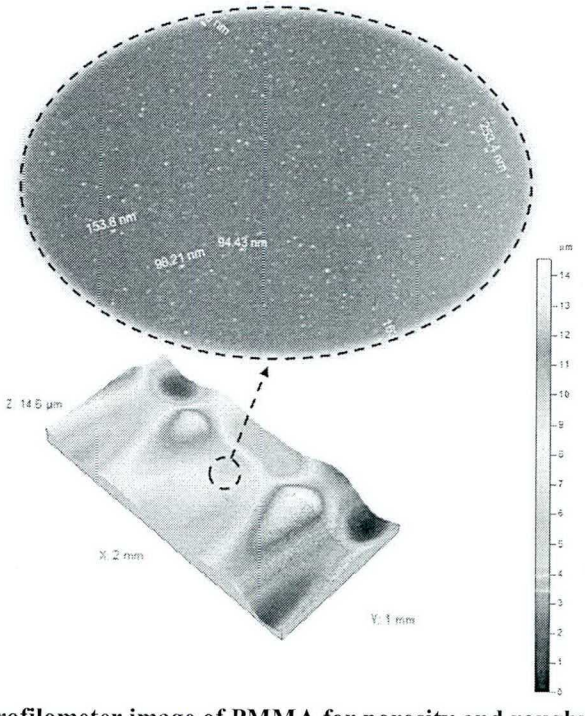

Fig. 6. FSEM and profilometer image of PMMA for porosity and roughness measurements.

can affect interactions between fluid and solid. The nozzle /diffuser elements, the chamber and the fluid reservoir were fabricated from PMMA. Drop shape analysis (DSA) was performed to determine the contact angle from the shadow image of a sessile drop and the surface tension or interfacial tension from the shadow image of a pendant drop. Drop shape analysis (DSA) was performed by KRÜSS (DSA100M, KRÜSS GmbH, Germany) measuring instruments with a sensitivity of 0.05°. This test was repeated 3 times at 20°C. The average of performed analysis of contact angle showed that a drop water was 58.36° (±2.85°). The results showed that the PMMA used in this study was hydrophilic and usual no-slip boundary condition was still valid. In other words, there is no self-filling and fluid flow due to the hydrophilic properties in flow tests. The DSA results are shown in Fig. 5.

3.2 Microscopic Image Investigation

Microscopic images were used to evaluate surface properties of micropump due to the possibility of testing with biological fluids in the future studies. As described in Section 2, the nozzle /diffuser elements, the chamber and the fluid reservoir were fabricated in clean room by the rapid prototyping device (Objet260 Connex3) with 16-micron layer resolution. Therefore, we examined a piece of the PMMA material in the field-emission scanning electron microscope (FSEM). Moreover, profilometer was used to visualize surface porosity and roughness characteristics of PMMA surface. In most cases, porosity and roughness are undesirable while, depending on the type of application, pore structures on the flow surface are preferred.

As shown in Fig. 6, undesired porosity was in the nanometer size, flow surface was completely assumed as smooth surface. In addition, the mean roughness was measured as 383.4 Å. Thereby, the undesired particles and the amount of the roughness of the PMMA surface have no effect on the fluid behavior of the chamber or the fluid in the nozzle/diffuser elements.

Another important issue was to determine the inlet and outlet diameters of the nozzle/diffuser elements

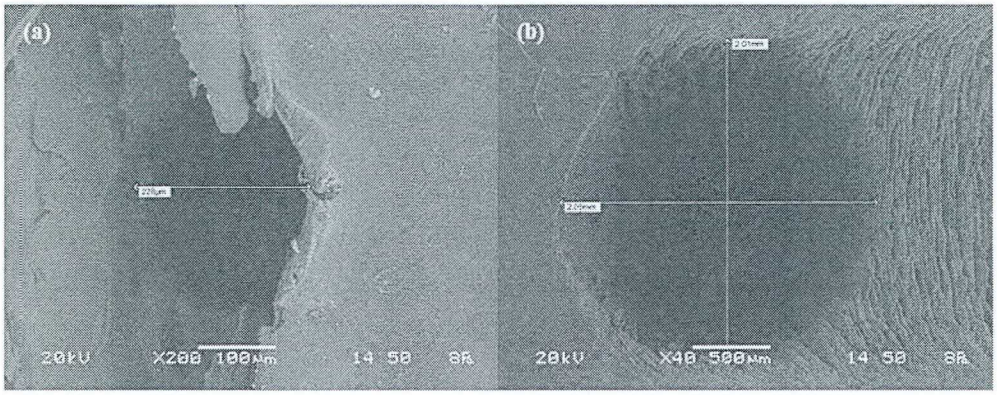

Fig. 7. A (SEM) images of PMMA (a) Nozzle/ diffuser inlet (b) Nozzle/ diffuser outlet.

in terms of the reliability of the calibration. Hydraulic diameters were designed as 0.2 mm and 2 mm, and SEM was used to determine the exact sizes after fabrication. Figure 7 shows the image of the Scanning Electron Microscope (SEM) of (a) water inlet and (b) outlet sections to these nozzle/diffuser elements. The water in the chamber is entered to the nozzle/ diffuser with a hydraulic diameter of 257.07 µm. Moreover, the diameter of nozzle/ diffuser element was 2061.91 µm at the moment of full water discharge. This causes at the discharge moment, the pressure to increase and the velocity to decrease.

3.3 Simulation Results of the Diaphragm Displacements

The piezoelectric crystal was used in both micropumps with a diameter of 14 mm and 0.2 mm thickness as an actuator. Silicon was also used as a diaphragm with a diameter of 25 mm and a thickness of 0.1 mm on each silicon diaphragm a piezoelectric was clamped. The voltage caused a vibration in the piezoelectric actuator. The piezoelectric edges were fully clamped on the silicon diaphragm. Therefore, the horizontal vibration was converted to the vertical vibration. The voltage determines the vibration amplitude and the frequency specifies the number of vibrations. The presented micropumps in this study were designed as potential candidate for biomedical applications which require relatively low level of driving voltages and frequencies. Thus, the driving voltage values were set to 5 V to 45 V by 5 V increments and the frequencies were 5 Hz, 10 Hz, 15 Hz and 20 Hz. Diaphragm displacement calculations were carried out by finite element methods. The Material, geometric shape and applied sinusoidal voltage were same in diaphragms, because of this diaphragm displacement was the same in SDM and BDM. Figure 8 shows the simulation results of diaphragm displacements at the moment of water discharge from the chamber. It shows that the increase in voltage increased displacement. Additionally, increasing the frequency reduced displacement. Thus, the piezoelectric vertical vibration or displacement mode depends on the applied AC voltage behavior. The piezoelectric displacement is transmitted exactly to the diaphragm because of being tangent. Finally, the diaphragm displacement causes the pressure difference in the chamber, and it causes fluid transport from reservoir to chamber and chamber to outlet. The net flow rate values of the proposed micropumps were shown in Section 3.4. However, the displacement results have 99% liner behavior. The maximum displacement was obtained 4.097 µm in 45 V and 5 Hz.

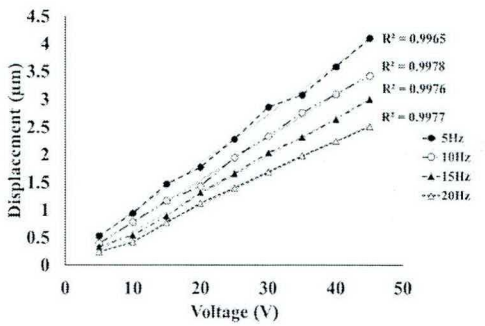

Fig. 8. Diaphragm displacement results at 5 Hz, 10 Hz, 15 Hz and 20 Hz.

3.4 Experimental Results of the Flow Rates

At the mentioned voltages and frequencies, we measured the net flow rate of the micropumps. Figure 9 shows the results of flow rates of SDM and BDM micropumps. The amplitude of the diaphragm displacement was increased by increasing the voltage. The frequency increase led to a decrease in displacement at per stroke. However, due to the increase in the number of vibrations, which is the total number of strokes, the flow rates in both micropump increased. There was linear correlation in Fig. 9, linear behavior of each pump at different driving frequencies were given according to experimental measurement. At all frequencies, the slope of the BDM was higher. So, with increasing voltage, the flow rates increase was higher compared to SDM. The maximum flow rates obtained for SDM and BDM in 45 V and 20 Hz were 32.58 ml/min and 35.4 ml/min respectively.

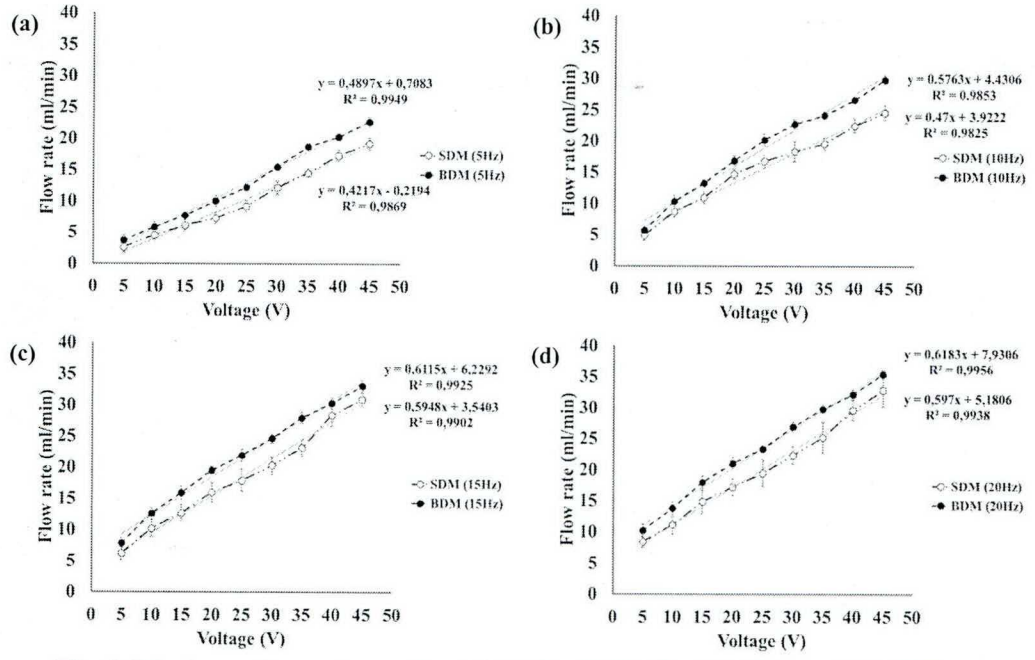

Fig. 9. Maximum flow rate results at (a) 5 Hz, (b) 10 Hz, (c) 15 Hz and (d) 20 Hz.

4. DISCUSSION

In this study, the performance of two novel micropumps was studied in the same experimental conditions. The only difference in the SDM and BDM was the number of vibrating diaphragms. Based on the results obtained in Section 3, the BDM flow rate compared to SDM at 5 Hz, 10 Hz, 15 Hz and 20 Hz were increased to 22%, 16.39%, 15.97% and 15.19% respectively. The water weight inside the chamber prevented moving the bottom diaphragm of the BDM. If the water weight force was not in the opposite direction of the bottom diaphragm force, we would expect a significant increase in the flow rate of the BDM design. As an important advantage, in the daily usage BDM design gives an opportunity to use both side facing upwards without losing the flow rate when the reservoir is closed to the atmosphere and adjustable according to the nozzle elements.

4.1 Comparison with the State of the Art

The presented micropumps in this study were designed as potential candidate for biomedical applications which require relatively low level of driving voltages and frequencies. Insulin delivery or other fluidic drugs dispersion into the human body might be possible by these micropump designs. Table 2 shows the similar studies about the piezoelectric micropumps and their flow rates during the last 10 years.

These studies include the micropumps with larger piezoelectric actuator and larger chambers. In addition, unlike our designs, they used higher voltages and frequencies. Thereby, some of the studies created higher flow rates.

When the studies in Table 2 were investigated, it was seen that Zhang *et al.* (2013a & 2013b), Pan *et al.* (2015), Okura *et al.* (2017) and Ye *et al.* (2018) used very high AC voltages between 150 V and 400 V. These driving AC voltage levels can be considered very high and risky when the micropumps were considered to be used near the body surface for biomedical related applications. In addition, all the studies mentioned above used a check-valve in their designs. In the study by Ma *et al.* (2015a), they used 70 V AC voltage at 25 Hz and they measured 196 ml/min net flow rate.

In their study, the diameter of PZT actuator was 2.5 time larger than we used in SDM and BDM micropump. Thereby, the maximum flow rate was almost 2.5 times higher according to our results. In fact, they did not show the calibration flow rate calculation and subtraction from the net flow rate values when the driving voltage was zero (at static condition). In addition, Ma *et al.* (2015b & 2016) used relatively low driving voltages (70-80 V) and frequency (20 Hz). But in these studies, they measured low net flow rates, i.e. 6.21 ml/min and 9.1 ml/min respectively. The most similar study to this presented study was done by Ma *et al.* (2016) with a valveless geometry. Even though they used similar size PZT actuator, their chamber height was 2.5 times bigger than our SDM and BDM micropump chambers. Thereby, they measured 2.5 times lower flow rates as compatible with the literature because of the chamber height effect (Lin *et al.*, 2006; Ni *et al.*, 2010).

When these studies are considered in general, we see that we have obtained a high flow rate at lower voltage and frequency values by using an integrated reservoir with SDM and BDM designs.

Table 2 Summaries of experimental studies and findings in open literature

Ref.	Valves type	Piezoelectrics and size (mm)	Chambers and size (mm)	Diaphragm material	Volt. (V)	Freq. (Hz)	Q (ml/min)
Zhang *et al.*, 2013a	Check valve	1 Φ35 mm	1 n/r	n/r	150	30	26.55
Zhang *et al.*, 2013b	Check valve	2 Φ35 mm	1 n/r	Unused	200	15	45.98
Wang *et al.*, 2014	Check valve	1 30×15×0.4	1 Φ 10mm	Rubber	400	490	105
Ma *et al.*, 2015a	Check valve	1 Φ35 mm	1 Φ34 mm	Unused	±70	25	196
Ma *et al.*, 2015b	Check valve	1 22×40×0.7	1 Φ 10mm	Silicon	80	20	6.21
Pan *et al.*, 2015	Check valve	1 110×20×0.8	1 20×20×13.7	Silicon	400	445.5	163.7
Ma *et al.*, 2016	Valveless	2 Φ 20mm	1 40×40×10	PT	±70	70	9.1
Okura *et al.*, 2017	Check valve	1 n/r	1 25×25×4.8	Resin	250	60	10
Ye *et al.*, 2018	Check valve	26 10×10×0.7	1 Φ 24mm	Kapton	400	750	187.2
SDM	Valveless	1 Φ 14mm	1 Φ 25mm	Silicon	45	20	32.85
BDM	Valveless	2 Φ 14mm	1 Φ 25mm	Silicon	45	20	35.4

4.2 Biomedical Considerations of Micropumps

Micropumps are one of the most important MEMS devices that can play an important role in drug delivering. The micropumps that are designed for the purpose of drug delivery should meet the requirements and basic terms, including drug biocompatibility, actuation safety, desired and controllable flow rate, small chip size and low power consumption. Biocompatibility is a very important key parameter that is necessarily considered for drug delivery micropumps (Lins *et al.*, 2001; Grayson *et al.*, 2004). On the other hand, the micropumps used for the purpose of drug delivery in the human body should be selected so that they had biocompatibility and biostability (Anderson *et al.*, 1999). Moreover, the implanted micropump based drug delivery system should have sufficient resistance to the physiological environment and the adverse impact of surrounding tissues (Anderson *et al.*, 2013).

Silicon is a good biocompatible material. It is one of the materials which has been much preferred in recent years' biomedical studies. However, the process of using polymers in medical fields is widespread and suitable for human implantation. Additionally, Polymer materials such as PMMA, PDMS, and SU-8 photo resist have better biocompatibility and are more preferred in micropump based drug delivery (Nisar *et al.*, 2008). It might be concluded that micropump designs in this study were compatible with medical considerations.

5. Conclusion

The purpose of this study was to investigate the effect of electro-mechanical factors on the flow rate. SDM and BDM were two novel designs that proposed in this study. The effect of voltage and frequency was clearly shown on the flow rates. The embedded reservoir combined with the chambers were presented promising results. Materials were biocompatible which considered as a crucial factor for biomedical applications. The flow rates were comparable with the state-of-the-art literature. The SDM flow rate was increased by 37.73% at 10 Hz, 47% at 15 Hz and 52.06% at 20 Hz compared to 5 Hz reference excitation frequency. Moreover, as for BDM flow rates, the increment rates were 33.70%, 42.90% and 47.93% for the same frequencies. Both SDM and BDM flow rates were linearly increased as a function of voltages at all frequencies. All in all, experimental results showed that our novel BDM design will be a good candidate especially for biomedical applications, such as drug delivery, blood transport after more investigations.

Acknowledgements

This study was supported by Scientific Research Projects Unit of Sakarya University of Applied Sciences (Project Number: 2017-50-02-026).

References

Afrasiab, H., M. Movahhedy and A. Assempour (2011). Proposal of a new design for valveless

micropumps. *Scientia Iranica* 18(6), 1261-1266.

Amirouche, F., Y. Zhou and T. Johnson (2009). Current micropump technologies and their biomedical applications. *Microsystem Technologies* 15(5), 647-666.

Anderson, J. M. (1999). Issues and perspectives on the biocompatibility and immunotoxicity evaluation of implanted controlled release systems. *Journal of Controlled Release* 57(2), 107-113.

Anderson, J. M. (2013). *Inflammation, Wound Healing, and the Foreign-Body Response. In: Biomaterials science*. Academic Press, USA.

Cazorla, P. H., O. Fuchs, M. Cochet, S. Maubert, G. L. Rhun, Y. Fouillet and E. Defay (2016). A low voltage silicon micro-pump based on piezoelectric thin films. *Sensors and Actuators A: Physical* 250, 35-39.

Chang, H. T., C. Y. Lee and C. Y. Wen (2006). Design and modeling of electromagnetic actuator in mems-based valveless impedance pump. *Microsystem Technologies* 13(11-12), 1615-1622.

Derakhshan, S., B. Beigzadeh, M. Rashidi and H. Pourrahmani (2019). Performance Improvement and Two-Phase Flow Study of a Piezoelectric Micropump with Tesla Nozzle-Diffuser Microvalves. *Journal of Applied Fluid Mechanics* 12(2), 341-350.

Dereshgi, H. A. (2016, November). Design of novel micro-pumps for mechatronic applications. *In 4th Int. Symposium on Innovative Technologies in Engineering and Science*, Antalya, Turkey.

Dereshgi, H. A. and M. Z. Yildiz (2018a). A novel micropump design: Investigation of the voltage effect on the net flow rate. *Sakarya University Journal of Science* 22(4), 1152-1156.

Dereshgi, H. A. and M. Z. Yildiz (2018b). Investigation of electro-mechanical factors effecting piezoelectric actuator for valveless micropump characteristics. *Journal of Engineering Science and Technology* 13(9), 2843-2856.

Dereshgi, H. A. and M. Z. Yildiz (2019, April). Numerical Study of Novel MEMS-Based Valveless Piezoelectric Micropumps in the Range of Low Voltages and Frequencies. *Scientific Meeting on Electrical-Electronics & Biomedical Engineering and Computer Science (EBBT)*, Istanbul, Turkey.

Dong, J. S., R. G. Liu, W. S. Liu, Q. Q. Chen, Y. Yang, Y. Wu, Z. G. Yang and B. S. Lin (2017). Design of a piezoelectric pump with dual vibrators. *Sensors and Actuators A: Physical* 257, 165–172.

Ehsani, A. and A. Nejat (2017). Conceptual design and performance analysis of a novel flexible-valve micropump using magneto-fluid–solid interaction. *Smart Materials and Structures* 26(5), 055036.

Farshchi Yazdi, S. A. F., A. Corigliano and R. Ardito (2019). 3-D Design and Simulation of a Piezoelectric Micropump. *Micromachines* 10(4), 259.

Grayson, A., R. Shawgo, A. Johnson, N. Flynn, Y. Li, M. Cima and R. Langer (2004). A BioMEMS Review: MEMS Technology for Physiologically Integrated Devices. *Proceedings of the IEEE* 92(1), 6-21.

Hamid, N. A., B. Y. Majlis, J. Yunas, A. R. Syafeeza, Y. C. Wong and M. Ibrahim (2016). A stack bonded thermo-pneumatic micro-pump utilizing polyimide based actuator membrane for biomedical applications. *Microsystem Technologies* 23(9), 4037-4043.

Holman, J. P. and W. J. Gajda (2001). *Experimental methods for engineers*. McGraw-Hill, New York, USA.

Hsu, Y. C., S. J. Lin and C. C. Hou (2007). Development of peristaltic antithrombogenic micropumps for in vitro and ex vivo blood transportation tests. *Microsystem Technologies* 14(1), 31-41.

Johnson, D. and D. Borkholder (2016). Towards an Implantable, Low Flow Micropump That Uses No Power in the Blocked-Flow State. *Micromachines* 7(6), 99.

Kawun, P., S. Leahy and Y. Lai (2016). A thin PDMS nozzle/diffuser micropump for biomedical applications. *Sensors and Actuators A: Physical* 249, 149-154.

Kolahdouz, E. M., K. Mohammadzadeh and E. Shirani (2014). Performance of piezoelectrically actuated micropump with different driving voltage shapes and frequencies. *Scientia Iranica. Transaction B, Mechanical Engineering* 21(5), 1635-1642.

Le, S. and H. Hegab (2017). Investigation of a multistage micro gas compressor cascaded in series for increase pressure rise. *Sensors and Actuators A: Physical* 256, 66-76.

Lee, C. Y., P. C. Chou, L. M. Fu and J. H. Zhong (2012, September). Design and fabrication of an electromagnetic pump for microfluidic applications. *IEEE Symposium on Industrial Electronics and Applications*, Bandung, Indonesia.

Lin, Q., B. Yang, J. Xie and Y. C. Tai (2006). Dynamic simulation of a peristaltic micropump considering coupled fluid flow and structural motion. *Journal of Micromechanics and Microengineering* 17(2), 220-228.

Lins, G. and L. Skogberg (2001). *An investigation of insulin pump therapy and evaluation of using a micropump in a future insulin pump*. M.S. thesis, KTH, Stockholm, Sweden.

Ma, H. K., R. H. Chen and Y. H. Hsu (2015a).

Development of a piezoelectric-driven miniature pump for biomedical applications. *Sensors and Actuators A: Physical* 234, 23-33.

Ma, H. K., R. H. Chen, N. S. Yu and Y. H. Hsu (2016). A miniature circular pump with a piezoelectric bimorph and a disposable chamber for biomedical applications. *Sensors and Actuators A: Physical* 251, 108-118.

Ma, H. K., W. F. Luo and J. Y. Lin (2015b). Development of a piezoelectric micropump with novel separable design for medical applications. *Sensors and Actuators A: Physical* 236, 57-66.

Maillefer, D., S. Gamper, B. Frehner, P. Balmer, H. V. Lintel and P. Renaud (2001). A high-performance silicon micropump for disposable drug delivery systems. *14th IEEE International Conference on Micro Electro Mechanical Systems (Cat. No.01CH37090)*.

Mohammadzadeh, K., E. M. Kolahdouz, E. Shirani and M. B. Shafii (2013). Numerical study on the performance of Tesla type microvalve in a valveless micropump in the range of low frequencies. *Journal of Micro-Bio Robotics* 8(3-4), 145-159.

Mohith, S., P. N. Karanth and S. M. Kulkarni (2019). Recent trends in mechanical micropumps and their applications: A review. *Mechatronics* 60, 34-55.

Ni, J., F. Huang, B. Wang, B. Li and Q. Lin (2010). A planar PDMS micropump using in-contact minimized-leakage check valves. *Journal of Micromechanics and Microengineering* 20(9), 095033.

Nisar, A., N. Afzulpurkar, B. Mahaisavariya and A. Tuantranont (2008). MEMS-based micropumps in drug delivery and biomedical applications. *Sensors and Actuators B: Chemical* 130(2), 917-942.

Okura, N., Y. Nakashoji, T. Koshirogane, M. Kondo, Y. Tanaka, K. Inoue and M. Hashimoto (2017). A compact and facile microfluidic droplet creation device using a piezoelectric diaphragm micropump for droplet digital PCR platforms. *Electrophoresis* 38(20), 2666-2672.

Pabst, O., J. Perelaer, E. Beckert, U. S. Schubert, R. Eberhardt and A. Tünnermann (2013). All inkjet-printed piezoelectric polymer actuators: Characterization and applications for micropumps in lab-on-a-chip systems. *Organic Electronics* 14(12), 3423-3429.

Pabst, O., S. Hölzer, E. Beckert, J. Perelaer, U. S. Schubert, R. Eberhardt and A. Tünnermann (2014). Inkjet printed micropump actuator based on piezoelectric polymers: Device performance and morphology studies. *Organic Electronics* 15(11), 3306-3315.

Pan, Q. S., L. G. He, F. S. Huang, X. Y. Wang and Z. H. Feng (2015). Piezoelectric micropump using dual-frequency drive. *Sensors and Actuators A: Physical* 229, 86–93.

Revathi, S. and R. Padmanabhan (2018). Design and Development of Piezoelectric Composite-Based Micropump. *Journal of Microelectromechanical Systems* 27(6), 1105-1113.

Robertson, J. M., R. X. Rodriguez, L. R. Holmes, P. T. Mather and E. D. Wetzel (2016). Thermally driven microfluidic pumping via reversible shape memory polymers. *Smart Materials and Structures* 25(8), 085043.

Sardar, V. B., N. R. Rajhans, A. Pathak and T. Prabhu (2016). Developments in silicone material for biomedical applications- A review. *14th International Conference on Humanizing Work and Work Environment HWWE*.

Schomburg, W. K., J. Vollmer, B. Bustgens, J. Fahrenberg, H. Hein and W. Menz (1994). Microfluidic components in LIGA technique. *Journal of Micromechanics and Microengineering* 4(4), 186-191.

Shaegh, S. A. M., Z. Wang, S. H. Ng, R. Wu, H. T. Nguyen, L. C. Z. Chan, A. G. G. Toh and Z. Wang (2015). Plug-and-play microvalve and micropump for rapid integration with microfluidic chips. *Microfluidics and Nanofluidics* 19(3), 557-564.

Shoji, E. (2016). Fabrication of a diaphragm micropump system utilizing the ionomer-based polymer actuator. *Sensors and Actuators B: Chemical* 237, 660-665.

Sim, W. Y., H. J. Yoon, O. C. Jeong and S. S. Yang (2003). A phase-change type micropump with aluminum flap valves. *Journal of Micromechanics and Microengineering* 13(2), 286-294.

Singh, S., N. Kumar, D. George and A. Sen (2015). Analytical modeling, simulations and experimental studies of a PZT actuated planar valveless PDMS micropump. *Sensors and Actuators A: Physical* 225, 81-94.

Singhal, V., S. V. Garimella and J. Y. Murthy (2004). Low Reynolds number flow through nozzle-diffuser elements in valveless micropumps. *Sensors and Actuators A: Physical* 113(2), 226-235.

Smits, J. G. and N. V. Vitafin (1984). Piezo-electrical micropump. *European patent EP0134614*.

Stemme, E. and G. Stemme (1993). A valveless diffuser/nozzle-based fluid pump. *Sensors and Actuators A: physical* 39(2), 159-167.

Tanaka, Y., Y. Noguchi, Y. Yalikun and N. Kamamichi (2017). Earthworm muscle driven bio-micropump. *Sensors and Actuators B: Chemical* 242, 1186-1192.

Tay, F. E. H. (2002). *Microfluidics and bioMEMS applications*. Boston: Kluwer Academic

Publishers, London, United Kingdom.

Teymoori, M. M. and E. Abbaspour-Sani (2005). Design and simulation of a novel electrostatic peristaltic micromachined pump for drug delivery applications. *Sensors and Actuators A: Physical* 117(2), 222-229.

Wang, J., Y. Liu, Y. Shen, S. Chen and Z. Yang (2016). A Resonant Piezoelectric Diaphragm Pump Transferring Gas with Compact Structure. *Micromachines* 7(12), 219.

Wang, X. Y., Y. T. Ma, G. Y. Yan, D. Huang and Z. H. Feng (2014). High flow-rate piezoelectric micropump with two fixed ends polydimethylsiloxane valves and compressible spaces. *Sensors and Actuators A: Physical* 218, 94-104.

Wang, Y. N. and L. M. Fu (2018). Micropumps and biomedical applications – A review. *Microelectronic Engineering* 195, 121-138.

Ye, Y., J. Chen, Y. J. Ren and Z. H. Feng (2018). Valve improvement for high flow rate piezoelectric pump with PDMS film valves. *Sensors and Actuators A: Physical* 283, 245-253.

Yildiz, M. Z. and H. A. Dereshgi (2019). Design of PZT micropumps for biomedical applications: Glaucoma treatment. *Journal of Engg. Research* 7(2), 226-241.

Zhang, Z., J. Kan, G. Cheng, H. Wang and Y. Jiang (2013a). A piezoelectric micropump with an integrated sensor based on space-division multiplexing. *Sensors and Actuators A: Physical* 203, 29-36.

Zhang, Z., J. Kan, S. Wang, H. Wang, J. Wen and Z. Ma (2013b). Flow rate self-sensing of a pump with double piezoelectric actuators. *Mechanical Systems and Signal Processing* 41(1-2), 639-648.

Zhou, Y. and F. Amirouche (2011). An Electromagnetically-Actuated All-PDMS Valveless Micropump for Drug Delivery. *Micromachines* 2(3), 345-355.